

Heriot-Watt University
Research Gateway

Experimental Measurement and Modeling of the Solubility of Methane in Methanol and Ethanol

Citation for published version:

Kapateh, MH, Chapoy, A, Burgass, RW & Tohidi Kalorazi, B 2016, 'Experimental Measurement and Modeling of the Solubility of Methane in Methanol and Ethanol', *Journal of Chemical and Engineering Data*, vol. 61, no. 1, pp. 666-673. <https://doi.org/10.1021/acs.jced.5b00793>

Digital Object Identifier (DOI):

[10.1021/acs.jced.5b00793](https://doi.org/10.1021/acs.jced.5b00793)

Link:

[Link to publication record in Heriot-Watt Research Portal](#)

Document Version:

Peer reviewed version

Published In:

Journal of Chemical and Engineering Data

General rights

Copyright for the publications made accessible via Heriot-Watt Research Portal is retained by the author(s) and / or other copyright owners and it is a condition of accessing these publications that users recognise and abide by the legal requirements associated with these rights.

Take down policy

Heriot-Watt University has made every reasonable effort to ensure that the content in Heriot-Watt Research Portal complies with UK legislation. If you believe that the public display of this file breaches copyright please contact open.access@hw.ac.uk providing details, and we will remove access to the work immediately and investigate your claim.

Experimental Measurement and Modeling of the Solubility of Methane in Methanol and Ethanol

Mahdi H Kapateh, Antonin Chapoy, Rod Burgass, Bahman Tohidi*

Hydrates, Flow Assurance & Phase Equilibria, Institute of Petroleum Engineering, Heriot Watt
University, EH14 4AS

Abstract

Knowledge of hydrate inhibitor distribution is essential for the economic operation of gas transportation and processing. A number of measurements were made to determine the solubility of methane, the main constituent in natural gas, in methanol and ethanol. Methanol and ethanol are two of the most commonly used gas hydrate inhibitors in the petroleum industry. The solubility data are essential in developing binary interaction parameters used in predicting inhibitor distribution in multi-component systems. The solubility of methane in methanol at 273.15 K and 1.1 to 47 MPa, and methane in ethanol at five different isotherms between 238.15 to 298.15 K and 0.3 to 41.7 MPa was measured. The results showed an average repeatability of 2.5% between the measured points. The results from the ethanol solubility measurements were used to optimize the interaction parameters of the CPA-SRK72 equation of state. The experimental data generated in this work are compared to literature data and to the calculations through the thermodynamic model tuned on our experimental data. The model calculations using a single binary interaction parameter was able to reproduce the new experimental with an absolute average deviation of 5.3% over the full data range, demonstrating the reliability of the approach.

Keywords

Gas Hydrates, Inhibitor, Inhibitor Distribution, Solubility, Methane, Methanol, Ethanol, Solubility, High Pressure, Low Temperature

Introduction

As the easily accessible oil and gas fields move towards their end of life production, dramatic changes have ensued in the petroleum industry with the advent of deep-water exploration. It is thus essential to ensure the un-interrupted production and transport of gas to the processing facilities. One of the major issues faced in such facilities is the production of natural gas hydrates at high pressure and low temperatures, making deep sea facilities a breeding ground for such issues. One of the most commonly used methodologies for hydrate prevention is the utilization of thermodynamic inhibitors. These are water soluble chemicals, typically alcohols. They reduce the water activity, thus shifting the hydrate phase boundary to lower temperatures and higher pressures. The common industrial practice is to use methanol, ethanol or Mono-ethylene glycol (MEG). Due to the high Capital Expenditure (CAPEX) and Operating Expenditure (OPEX) of hydrate inhibitor injection, it is essential for operators to be able to make accurate calculations using their thermodynamic models. Thus this study focused on the measurement of the solubility of methane (CH_4) in pure methanol and ethanol which were then used to optimize the binary interaction parameters between methane and the alcohols. These are essential for developing thermodynamic models capable of predicting inhibitor distribution in multi-component systems. The model was then used to predict the methanol and ethanol distribution in the methane rich phase (inhibitor loss). The data from this work may be used to develop binary interaction parameters and optimize the classical and statistical models used by operators.

Yarym-agaev et al. conducted a number of solubility measurements for CH_4 in methanol at 298.15 to 338.15 K and 2.5 to 12.5 MPa. ¹ Brunner et al. completed one the most extensive studies of CH_4 solubility in methanol and Methanol in CH_4 with measurements at 298.15 to 373.15 K and 3 to 100 MPa. ² Hong et al. also made a similar significant contribution to solubility data for

methanol in CH₄ making measurements between 200 to 330 K and 0.6 to 41.3 MPa. ³ Schneider measured the solubility of CH₄ in methanol in his PhD thesis at 183.15 to 298.15 and 0.9 to 10.3 MPa. ⁴ Ukai et al. measured CH₄ in methanol solubility at 280.15 K and the pressure ranges of 2.1 to 11.4 MPa. ⁵ Wang et al. made a number of solubility measurements at 283.2 to 303.2 K and 5 to 40 MPa. ⁶ Frost et al. also made a number of measurements recently at 298.87 K and 5 to 18 MPa. ⁷

The literature data for the solubility of CH₄ in ethanol are rather scarce. Suzuki et al. made a limited number of measurements at 313.4 to 333.4 K and 1.8 to 10.5 MPa. ⁸ Brunner et al. made a number of measurements at 298.15 to 498.15 K and 3.3 to 31.5 MPa. ⁹ Ukai et al. made measurements at 280.15 K and 1.5 to 5.7 MPa. ⁵ Friend et al. also made measurements at 323 to 373 K and 2.1 to 2.7 MPa. ¹⁰

As clearly apparent from the literature review, the availability of solubility data for CH₄ in ethanol in open literature is limited, particularly at the hydrate inhibition temperatures and pressures. Thus this study's main focus was the measurement and modeling of CH₄ in Ethanol at low temperatures and a wide range of pressures. This is of particular importance in the modern petroleum industry where there is a move towards the use of greener, less toxic chemicals. It is also of interest to petroleum companies operating in South America where an abundance of ethanol makes its use far more economically viable than other inhibitors. ¹¹⁻¹⁴

Materials and Method

Schematics of the set-up used for the solubility study is shown in Figure 1 and Figure 2. The rig was loaded with an alcohol and the cell was vacuumed to minimize the interference of air on the measurements. A pressurized cylinder containing CH₄ was then used to load the rig to the desired pressure. The details of the material used may be found in Table 1.

Table 1 Materials, their purity and suppliers used.

Chemical Name	Source	Mole Fraction Purity ^a	Purity Certification	Analysis method ^b
Methanol	J.T. Baker	0.9980	Avantor Materials	GC
Ethanol	J.T. Baker	0.9990	Avantor Materials	GC
Methane	BOC	0.9999	BOC Certified	GC

^a No additional purification is carried out for all samples. ^b GC: Gas Chromatography

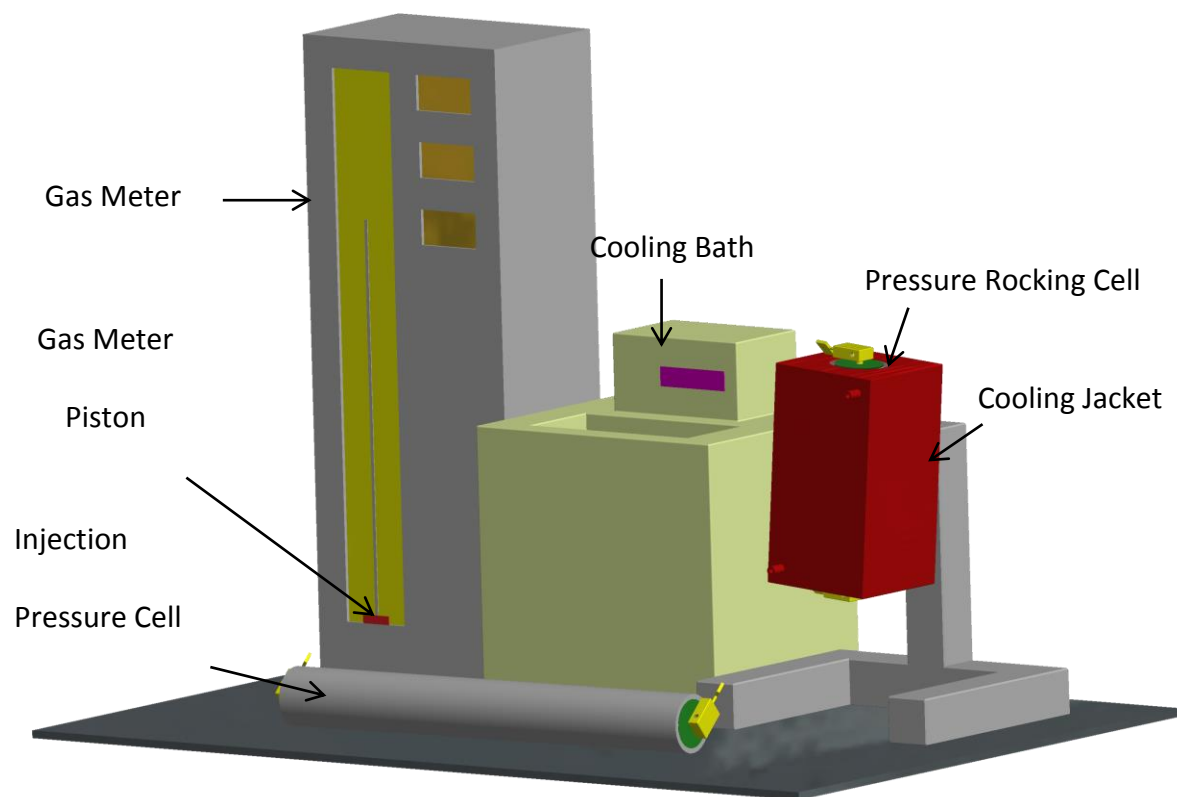


Figure 1 3D schematic of the pressure rig used in this work.

The setup used in this work was similar to the rocking cell setup used by Chapoy et al.¹⁵ to determine the saturation pressure of a multicomponent mixture.

The 350 cm³ (piston-less) pressure rocking cell was loaded with 300 cm³ of the desired alcohol from the top. The cell was then sealed. The air was vacuumed from the cell top via V02. The gas was injected into the cell from the top via V02. The gas cylinder was then disconnected and the pneumatic rocking cell was initialized, allowing the mixture to equilibrate (steady pressure and temperature on the computer log).

To measure the solubility of CH₄ in the solution at the specified pressure and temperature, a flash tank was connected to a VINCI Technology manual gas meter. The gas meter utilized, was capable of retaining a maximum capacity of 4000 cm³, with a volume and temperature resolution of 0.1 cm³ and 0.1 °C, respectively and a standard uncertainty of 0.1%.

For each measurement, the pressure and temperature of the cell, together with the pressure, temperature and initial volume of the gas meter chamber were recorded. The pressure of the cell in the rig was kept constant during sampling by CH₄ injection (V02). A liquid sample (average of 10 grams per run) was then passed from the base of the cell (V03), whilst it was held in a vertical position, into the 2-phase separator releasing the gas at atmospheric pressure into the gas meter (V05). By this means the CH₄ was collected in the gas meter. After all of the CH₄ was collected the volume was adjusted manually to give atmospheric pressure. The final volume at atmospheric pressure, together with temperature was recorded. The mass of the extracted solution was also measured using a Mettler Toledo balance with a weighing range of 0.5 – 3100 g, a resolution of 0.01 g and a standard uncertainty of $u(m) = 0.01$ g. The pressure and temperature of the gas meter were used to obtain the density of CH₄ at each point (relative standard uncertainty $u_r(\rho) = 0.0003$), which were then used to calculate the mole of CH₄ in the vapor phase. See Eq. 5 in Appendix A for the solubility calculation formula.

The pressure of the cell was increased by CH₄ injection from V01 and V02, and the procedure repeated, producing solubility results at various pressures and at a specific temperature.

The standard uncertainty of the pressure rocking cell transducer $u(P) = 0.04$ MPa and the standard uncertainty for the PRT temperature probe was $u(T) = 0.05$ K, the effects of which had negligible effect on the overall standard uncertainty of the measurements.

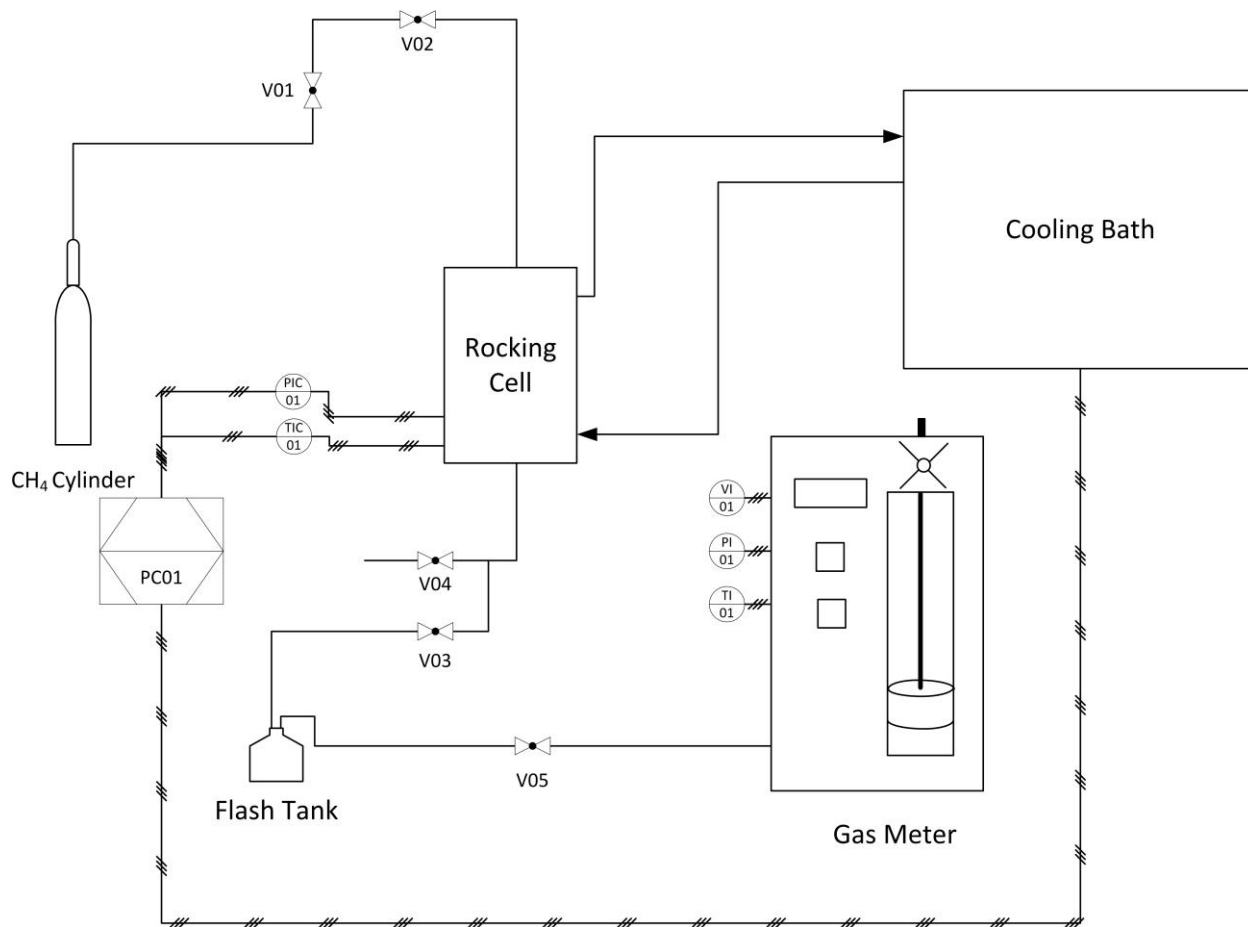


Figure 2 Schematic of the rocking cell setup used to measure the solubility of CH₄ in Alcohols.

Table 2 shows the key for this schematic.

Table 2 Key for Figure 2.

Key	Description
PI01	Gas Meter Pressure Indicator

PIC01	Equilibrium Cell Pressure Indicator/logger
TI01	Gas Meter Temperature Indicator
TIC01	Equilibrium Cell Temperature Indicator Controller
V01	CH ₄ Cylinder Control Valve
V02	Equilibrium Cell Injection Valve
V03	Equilibrium Cell Drain Valve
V04	Equilibrium Cell Drain Valve (Backup)
V05	Gas Meter Inlet Valve
VI01	Gas Meter Volume Indicator

Thermodynamic Modeling

A detailed description of the original thermodynamic model used in this work can be found elsewhere ^{16–18}. The thermodynamic model is based on the uniformity of fugacity of each component throughout all the phases. The CPA-SRK72 EoS was used throughout this work to determine the component fugacities in fluid phases.

The Cubic-Plus Association (CPA-SRK72) developed by Kontogeorgis et al. ¹⁹ combines the original SRK EoS developed by Soave ²⁰ and an associating term. The EoS is described in terms of compressibility factors, Z as:

Eq. 1 is the CPA-SRK72 EoS in terms of compressibility factors

$$Z^{CPA} = Z^{SRK} + Z^{Assoc} \quad (1)$$

Eq. 22222 is the Compressibility factor from the Soave-Redlich-Kwong EoS

$$Z^{SRK} = \frac{v}{v-b} - \frac{a}{RT(v+b)} \quad (2)$$

Eq. 3 is the compressibility factor from the association term

$$Z^{Assoc} = -\frac{1}{2} \left(1 + \rho \frac{\partial \ln g}{\partial \rho} \right) \sum_i \sum_{A_i} x_i (1 - X^{A_i}) \quad (3)$$

Where v is the molar volume, X^{A_i} is the mole fraction of the molecule i not bonded to site A and x_i is the superficial mole fraction of component i .

The CPA-SRK72 equation used in this work uses a simplified-hard sphere.²¹

The binary interaction parameters (BIPs) between methane and ethanol were adjusted using the solubility data mentioned previously and the new measured data through a Simplex algorithm using the objective function, OF , displayed in Eq. 4 (BIPs for methanol were reported by Haghighi et al.¹⁶):

Eq. 4 is the simplex algorithm using an objective function.²²

$$OF = \frac{1}{N} \sum_1^N \left| \frac{x_{exp} - x_{cal}}{x_{exp}} \right| \quad (4)$$

Where x is the solubility of methane in ethanol, N is the number of data points. The optimized BIPs for the CPA-SRK72-EoS over the considered temperatures is -0.049.

Results and Discussion

Table 3 demonstrates the measured solubility of methane in methanol. Table 4 show the measured solubility of methane in Ethanol, where T is temperature in kelvin, P is the pressure in MPa and x_i is the moles of CH_4 in the alcohol. Both tables also contain a number of the measurements repeated at the same pressure or in close proximity of the previously measured pressure. Based on the illustrated results the average percentage repeatability was calculated to be

$\pm 2.5\%$. The standard uncertainty of the measurements were calculated based on the four main variables within the measurements, the volume of methane measured using the gas meter, the mass of methanol and ethanol measured using the balance, the error inflicted by the calculation of alcohol in the atmospheric vapor phase, the mole fraction of CH_4 in the liquid phase using the CPA-SRK72 EoS and the repeatability. The standard uncertainty in the density data from NIST was deemed negligible at $u(\rho) = 0.0003$. The apparatus measurement standard uncertainties reported by the manufacturers were then used to calculate the uncertainty of each measurement (Appendix A). These showed an overall standard uncertainty of $u(x_i) = 0.029$ and $u(x_i) = 0.027$ for the solubility of CH_4 in Methanol and Ethanol respectively. Figure 3 shows the measured solubility of methane in Methanol at 273.15 K from this work along with the solubility measurements performed by Schneider and Hong et al.^{3,4} and model calculations demonstrating the model and literature data's agreement with the solubility measurements in this work. As can be seen from Figure 3 the experimental data set is in good agreement, demonstrating the reliability of the methods and equipment used in this work. It also illustrates the model calculations using the CPA-SRK72 EoS. The model was optimized for CH_4 in Methanol during a previous study Haghighi et al.¹⁶ using numerous data points from literature. Figure 4 shows the solubility of CH_4 in Methanol at 5 different isotherms measured by Hong et al.³ and the CPA-SRK72 model calculations for each isotherm. As can be seen, the model calculation is in good agreement with the experimental results. Figure 5 shows the CH_4 in Methanol solubility measurements by Brunner et al, Schneider and Yarym-Agaev et al.^{1,2,4} at 298.15 K in conjunction with the CPA-SRK72 model calculations, showing very good agreement between the calculations and the experimental measurements by the three sets of data. Figure 6 and Figure 7 show the solubility of Methanol in CH_4 at 273.15 and 298.15 K measured by Brunner et al., Krichevsky and Koroleva, Yarym-Agaev et al,

Hemmaplardh and King and Hong et al ^{1-3,23,24} together with the CPA-SRK72 model predictions. As demonstrated the predictions are in good agreement with the experimental results at lower pressures however as the pressure increases the model consistently under predicts the solubility. Figure 8 illustrates the solubility of methane in ethanol at 298.15 K measured in this work together with the measurements by Brunner et al ⁹, and unadjusted and adjusted CPA-SRK72 model predictions. The model's k_{ij} binary interaction parameters were adjusted using the measured experimental results in this work as no major source of solubility data for CH₄ in ethanol could be found by the author. The measurements conducted within this work were also in good agreement with the measurements by Brunner et al. ⁹. Figure 9 shows the solubility measurements from this work together with un-optimized and optimized CPA-SRK72 model predictions at five different isotherms. The predictions were in good agreement with the measured data after optimization. The model's binary interaction parameters were tuned on the experimental data from this work due to scarcity of experimental results in the open literature. Figure 10 shows the solubility of Ethanol in CH₄ at 298.15 K measured by Brunner et al. ⁹ together with the optimized and un-optimized CPA-SRK72 Model predictions. The model's binary interaction parameters were optimized on solubility, using the measured data during this work.

Table 3: Solubility of Methane in Methanol x_i at Temperature T, various pressures P and standard uncertainty in moles for each measurement, $u_c(x_i)$ ^a.

T/K	P/ MPa	x_i	$u_c(x_i)$
273.15	1.71	0.0172	0.0005
273.15	3.83	0.0350	0.0010
273.15	6.68	0.0536	0.0015
273.15	8.92	0.0772	0.0021

273.15	10.96	0.0925	0.0025
273.15	14.02	0.1175	0.0034
273.15	17.53	0.1324	0.0037
273.15	22.47	0.1569	0.0043
273.15	38.33	0.2193	0.0059
273.15	46.99	0.2578	0.0071

^a Standard uncertainties u are at $u_r(x_i) = 0.029$, $u(T) = 0.05$ K and $u(P) = 0.04$ MPa.

Table 4 Solubility of Methane in Ethanol x_i at Temperature T , various pressures P and standard uncertainty in moles for each measurement, $u_c(x_i)$ ^a.

T/K	P/ MPa	x_i	$u_c(x_i)$
238.15	0.786	0.0183	0.001
238.15	0.793	0.0172	0.001
238.15	1.365	0.0284	0.001
238.15	1.365	0.0280	0.001
238.15	2.944	0.0588	0.002
238.15	2.951	0.0561	0.001
238.15	5.254	0.0960	0.002
238.15	5.254	0.0974	0.003
238.15	8.246	0.1408	0.004
238.15	8.267	0.1407	0.004
238.15	16.175	0.2131	0.005
238.15	16.175	0.2103	0.005
238.15	24.159	0.2684	0.007
238.15	24.214	0.2716	0.007
238.15	31.488	0.3067	0.008
253.15	0.372	0.0092	0.000

253.15	0.372	0.0088	0.000
253.15	1.379	0.0243	0.001
253.15	1.379	0.0261	0.001
253.15	8.446	0.1290	0.003
253.15	8.460	0.1250	0.003
253.15	13.245	0.1790	0.005
253.15	13.334	0.1748	0.005
253.15	19.802	0.2293	0.006
253.15	19.850	0.2289	0.006
253.15	27.386	0.2732	0.007
253.15	27.414	0.2698	0.007
253.15	34.295	0.3077	0.008
253.15	34.329	0.3148	0.008
253.15	39.817	0.3293	0.008
263.15	0.331	0.0083	0.000
263.15	0.683	0.0132	0.000
263.15	0.689	0.0120	0.000
263.15	2.751	0.0432	0.001
263.15	2.758	0.0442	0.001
263.15	6.812	0.0997	0.003
263.15	6.819	0.0972	0.003
263.15	11.445	0.1500	0.004
263.15	11.445	0.1526	0.004
263.15	13.300	0.1796	0.005
263.15	13.838	0.1770	0.005
263.15	19.071	0.2143	0.006
263.15	19.078	0.2137	0.005

263.15	25.455	0.2589	0.007
263.15	25.511	0.2549	0.007
263.15	32.985	0.3015	0.008
263.15	33.060	0.3040	0.008
263.15	39.424	0.3363	0.009
273.15	2.296	0.0332	0.001
273.15	5.164	0.0714	0.001
273.15	10.563	0.1244	0.002
273.15	13.072	0.1501	0.003
273.15	17.202	0.1944	0.004
273.15	21.712	0.2352	0.005
273.15	28.406	0.2715	0.006
273.15	32.081	0.2958	0.007
273.15	36.639	0.3256	0.008
273.15	41.189	0.3490	0.008
298.15	0.641	0.0116	0.009
298.15	2.537	0.0234	0.000
298.15	4.316	0.0530	0.000
298.15	8.094	0.0927	0.001
298.15	11.356	0.1268	0.001
298.15	15.582	0.1674	0.002
298.15	21.029	0.2191	0.003
298.15	28.992	0.2707	0.004
298.15	35.170	0.3229	0.006
298.15	41.693	0.3535	0.007

^a Standard uncertainties u are at $u_r(x_i) = 0.029$, $u(T) = 0.05$ K and $u(P) = 0.04$ MPa.

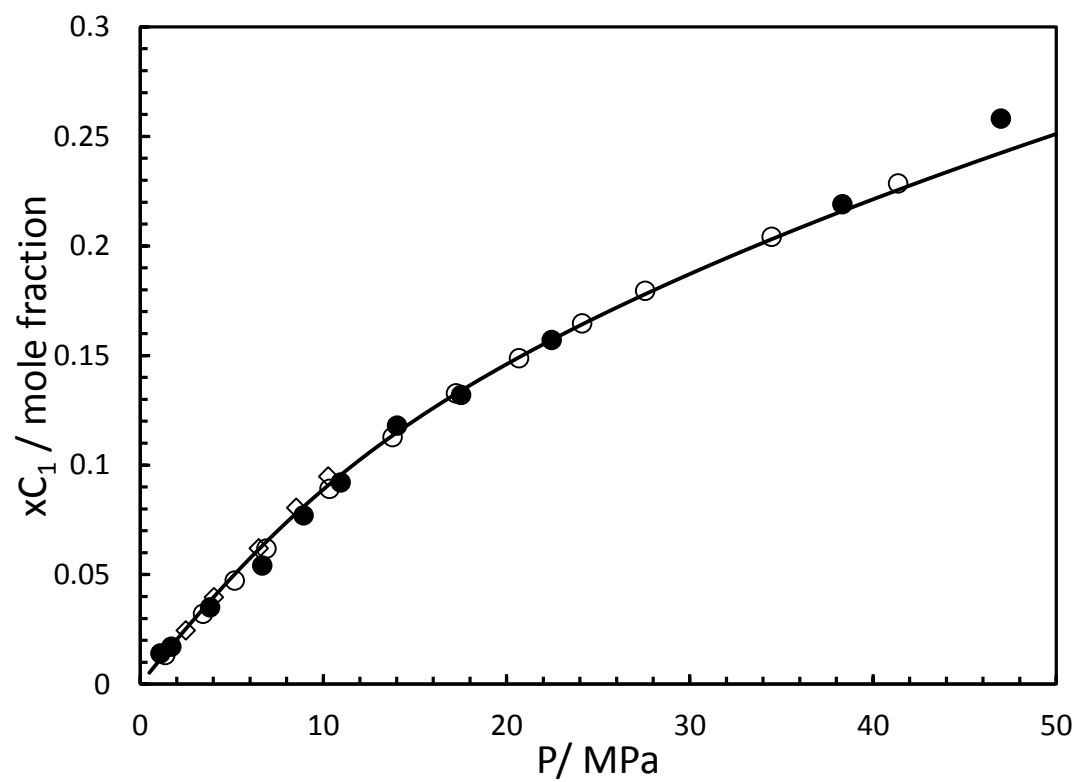


Figure 3. Methane Solubility in Methanol at 273.15 K. (●), this work; (◇) data from Schneider, 1978⁴; (○) data from Hong et al., 1987³. Black Line: CPA-SRK72-model

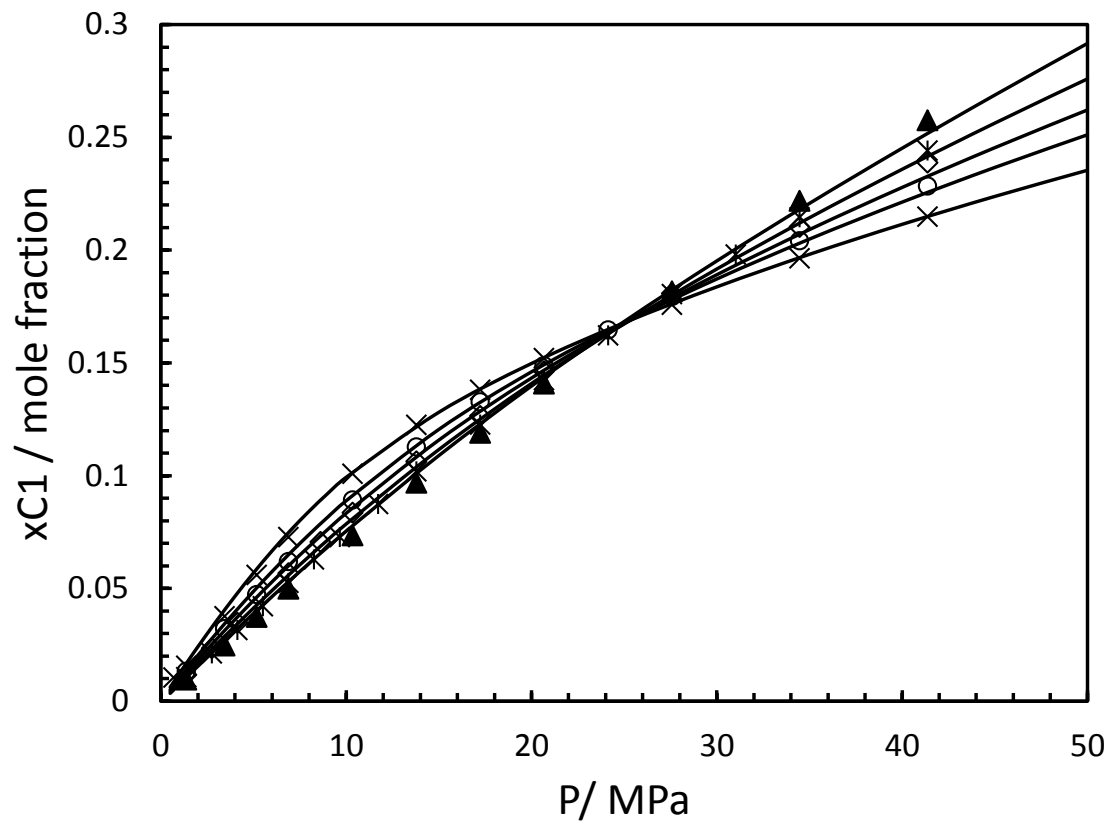


Figure 4. Methane Solubility in Methanol at (×) 250 , (○) 273.15 , (◇) 290 , (*) 310 and (▲) 330 K. data from Hong et al., 1987³. Black Line: CPA-SRK72-model

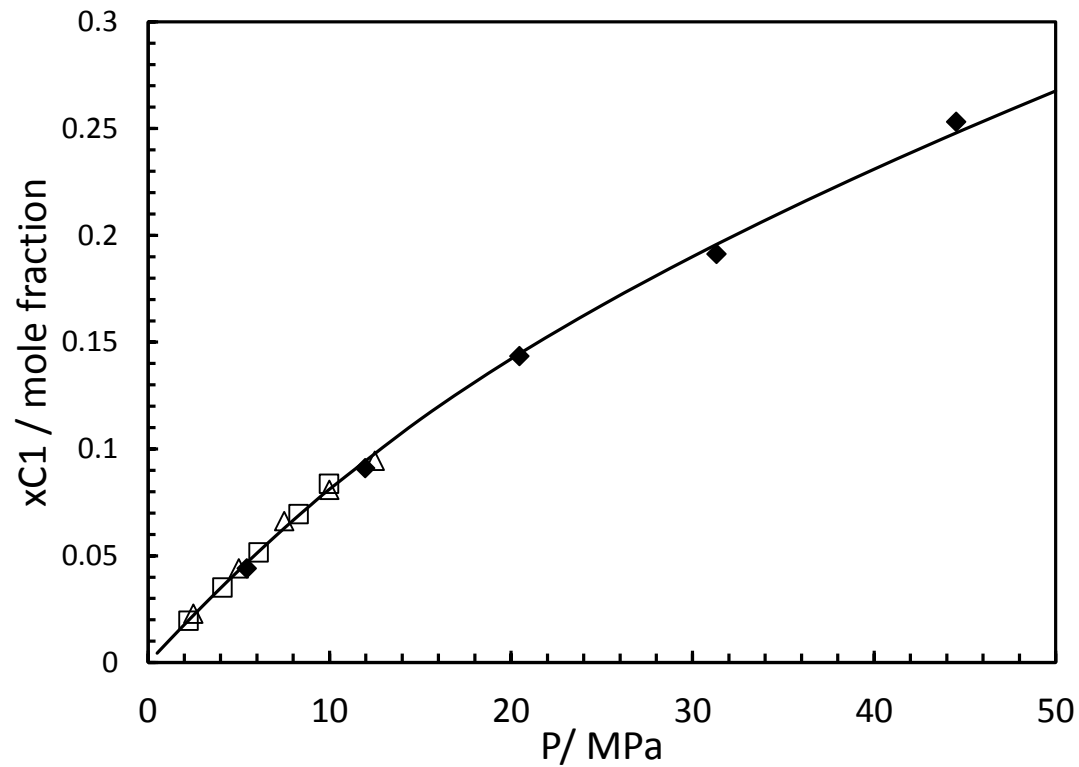


Figure 5. Methane Solubility in Methanol at 298.15 K. (◆), Brunner et al., 1987; (□) data from Schneider, 1978 ; (△) data from Yarym-Agaev et al., 1985 ^{1,2,4}. Black Line: CPA-SRK72-model.

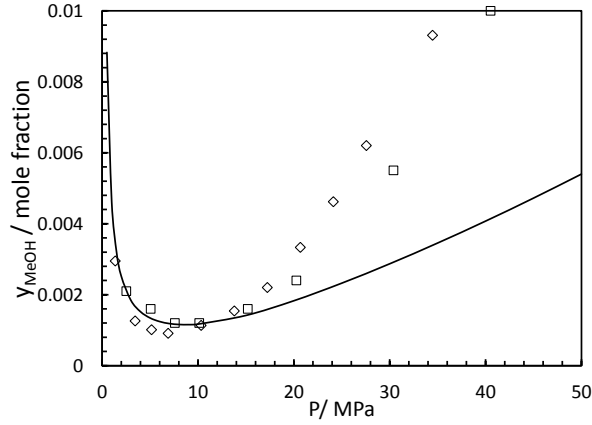


Figure 6. Methanol Solubility in Methane at 273.15 K. (\square) data from Krichevsky and Koroleva, 1941²⁴; (\diamond) data from Hong et al. (1987)³. Black Line: CPA-SRK72-model.

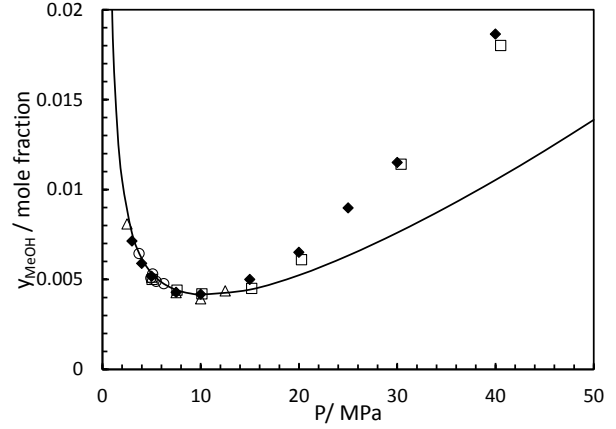


Figure 7. Methanol Solubility in Methane 298.15 K. (\blacklozenge), Brunner et al., 1987; (\square) data from Krichevsky and Koroleva, 1941 ; (\triangle) data from Yarym-Agaev et al., 1985 ; (\circ) data from Hemmaplardh and King (1972);^{1,2,23,24}. Black Lines: CPA-SRK72-model.

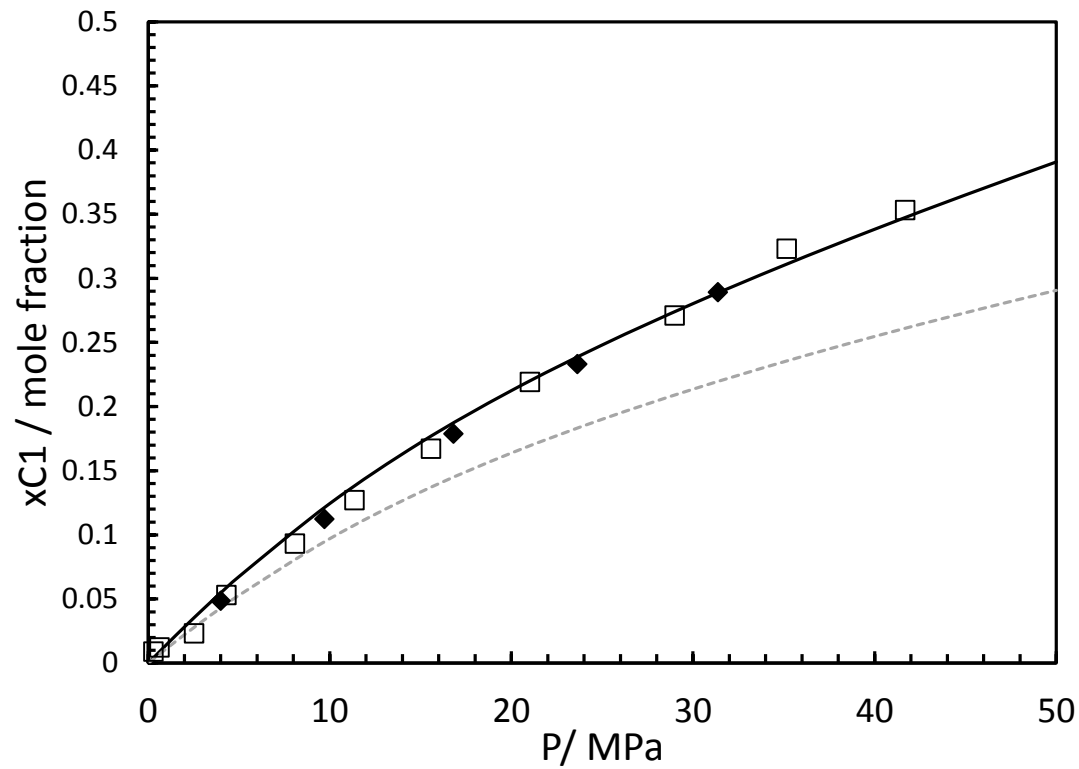


Figure 8. Methane Solubility in Ethanol at 298.15 K. (◆), Brunner et al., 1990⁹; (□) This work.

Lines: CPA-SRK72-model - Black lines: adjusted $k_{ij} = -0.049$; Dotted grey lines: $k_{ij} = 0$.

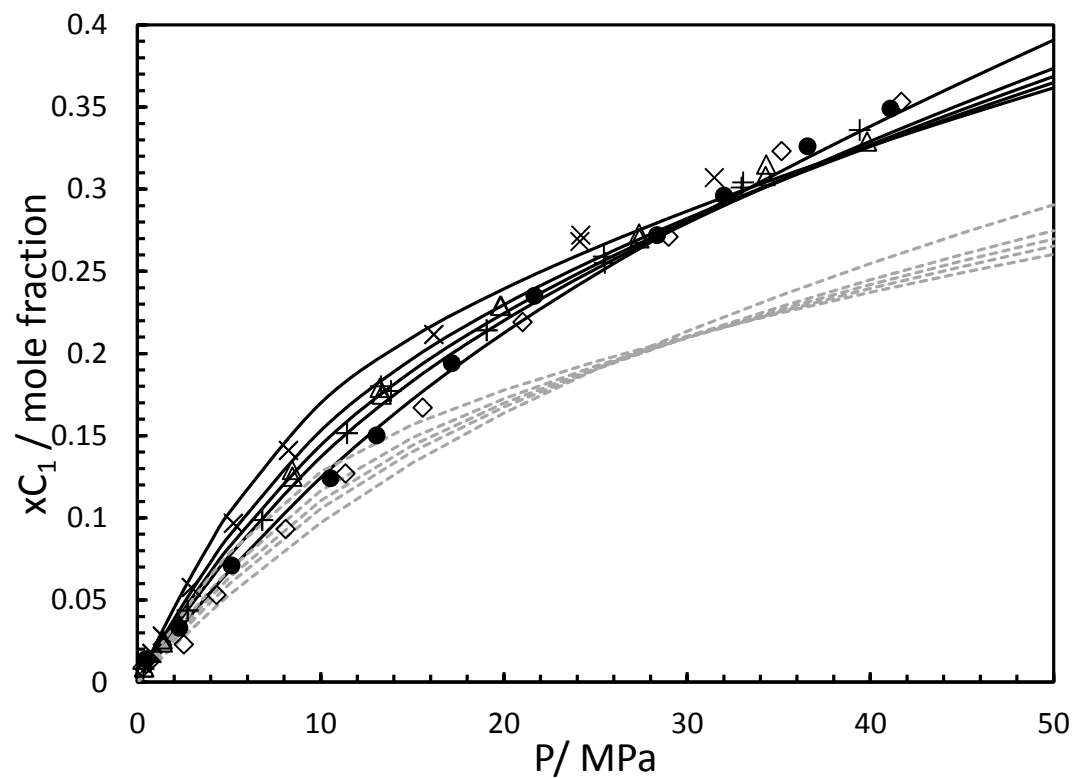


Figure 9. Methane Solubility in Ethanol at various temperatures. (×), 238.15 K; (Δ), 253.15 K; (+), 263.15 K; (●), 273.15 K; (◇), 298.15 K. Lines: CPA-SRK72-model - Black lines: adjusted $k_{ij} = -0.049$; Dotted grey lines: $k_{ij} = 0$.

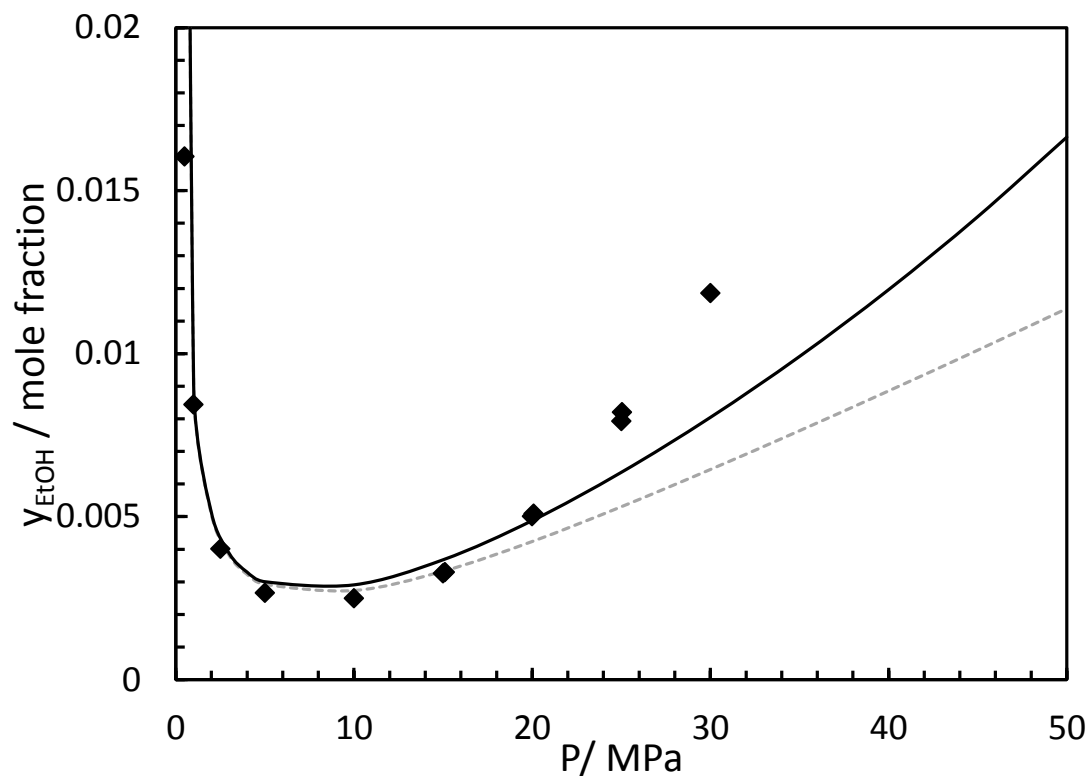


Figure 10. Ethanol Solubility in Methane at 298.15 K. (◆), Brunner et al., 1990⁹. Lines: CPA-SRK72-model - Black lines: adjusted $k_{ij} = -0.049$ (on solubility); Dotted grey lines: $k_{ij} = 0$.

Conclusion

Methanol and Ethanol are commonly used hydrate inhibitors by a number of oil and gas operators. Due to the lack of data in open literature for the temperature range required in hydrate prevention the experimental measurements in this work were mainly focused on the solubility of methane in ethanol. The solubility CH_4 in methanol showed good agreement with the data published in open literature thus demonstrating the reliability of the equipment and methods used in this work. Overall the modeling predictions showed an absolute average deviation of 5.31%.

Appendix A – Uncertainty Calculations

This section describes the calculations undertaken for the uncertainty analysis. Table 5 describes the various parameters used in the equations in the appendix.

Eq. 5 is used to calculate the solubility of CH₄ in the alcohol.

$$x_i = \frac{\left[mol_{CH_4}^v + mol_{CH_4}^l \right] - mol_{EtOH}^v}{mol_{EtOH}^l + mol_{EtOH}^v + mol_{CH_4}^v + mol_{CH_4}^l} \quad (5)$$

Eq. 6 demonstrates the solubility calculation in respect to the volume measured.

$$x_i = \frac{\left[(v_{CH_4} \times \rho_{CH_4}) + mol_{CH_4}^l \right] - mol_{EtOH}^v}{mol_{EtOH}^l + mol_{EtOH}^v + (v_{CH_4} \times \rho_{CH_4}) + mol_{CH_4}^l} \quad (6)$$

Eq. 7 is the derivative of the solubility equation with respect to volume, v.

$$\frac{\partial x_i}{\partial v} = \frac{\rho_{CH_4} (2 \times mol_{EtOH}^v + mol_{EtOH}^l)}{\left[(v_{CH_4} \times \rho_{CH_4}) + mol_{CH_4}^l + mol_{EtOH}^v + mol_{EtOH}^l \right]^2} \quad (7)$$

Eq. 8 shows the solubility equation with respect to mass, m.

$$x_i = \frac{mol_{CH_4}^v + \left(mol_{fracCH_4}^l \times \frac{m_{EtOH}}{46} \right) - mol_{EtOH}^v}{\frac{m_{EtOH}}{46} + mol_{EtOH}^v + mol_{CH_4}^v + \left(mol_{fracCH_4}^l \times \frac{m_{EtOH}}{46} \right)} \quad (8)$$

Eq. 9 shows the derivative of the solubility equation with respect to mass.

$$\frac{\partial x_i}{\partial m} = \frac{46 \left(-mol_{CH_4}^v + \left[2 \times mol_{fracCH_4}^l \times mol_{EtOH}^v \right] + mol_{EtOH}^v \right)}{\left[\left(46 \times mol_{CH_4}^v \right) + \left(mol_{fracCH_4}^l \times m \right) + \left(46 \times mol_{EtOH}^v \right) + m \right]^2} \quad (9)$$

Eq. 10 shows the solubility equation with respect to the mole fraction of CH₄ in liquid ethanol at atmospheric pressure.

$$x_i = \frac{mol_{CH_4}^v + [mol_{CH_4}^{frac} \times mol_{EtOH}^l] - mol_{EtOH}^v}{mol_{EtOH}^l + mol_{EtOH}^v + [mol_{CH_4}^v + [mol_{CH_4}^{frac} \times mol_{EtOH}^l]]} \quad (10)$$

Eq. 11 shows the derivative of the equation with respect to the mole fraction of CH₄ in liquid ethanol at atmospheric pressure.

$$\frac{\partial x_i}{\partial mol_{CH_4}^{frac}} = \frac{mol_{EtOH}^l (mol_{EtOH}^l + [2 \times mol_{EtOH}^v])}{[mol_{CH_4}^v + (mol_{EtOH}^l \times mol_{CH_4}^{frac}) + mol_{EtOH}^l + mol_{EtOH}^v]^2} \quad (11)$$

Eq. 12 shows the solubility equation with respect to the mole fraction of ethanol in gaseous CH₄ phase at atmospheric pressure.

$$x_i = \frac{mol_{CH_4}^v + mol_{CH_4}^l - [mol_{EtOH}^{frac} \times mol_{CH_4}^v]}{mol_{EtOH}^l + [mol_{EtOH}^{frac} \times mol_{CH_4}^v] + mol_{CH_4}^v + mol_{CH_4}^l} \quad (12)$$

Eq. 13 shows the derivative of the equation with respect to the mole fraction of ethanol in gaseous CH₄ phase at atmospheric pressure.

$$\frac{\partial x_i}{\partial mol_{EtOH}^{frac}} = \frac{mol_{CH_4}^v (2 \times mol_{CH_4}^v + 2 \times mol_{CH_4}^l + mol_{EtOH}^l)}{[(mol_{CH_4}^v \times mol_{EtOH}^{frac}) + mol_{CH_4}^v + mol_{CH_4}^l mol_{EtOH}^l]^2} \quad (13)$$

Standard uncertainty in gas meter volume measurements, $u(v) = 0.0005$ liters

Relative standard uncertainty in balance $u_r(m) = 0.005$

$u_r(mol_{CH_4}^{frac})$ = Relative standard uncertainty in CPA-SRK72 mol fraction calculation

(optimized) of CH₄ in Liquid = 0.05

$u_r(mol_{EtOH}^{frac})$ = Relative standard uncertainty in CPA-SRK72 mol fraction calculation

(optimized – limited data) of alcohol in CH₄ = 0.05

Standard uncertainty in NIST CH₄ density $u_r(\rho) = 0.0003$ (deemed negligible)

Standard uncertainty due to random error (repeatability), $u_{rep}(x_i) = 0.025$

Eq. 14 Cumulative uncertainty equation

$$u(x_i) = \sqrt{\left(\left(\frac{\partial x_i}{\partial v} \right)^2 \times u(v)^2 + \left(\frac{\partial x_i}{\partial m} \right)^2 \times u(m)^2 \right) + \left(\frac{\partial x_i}{\partial mol_{CH_4}^{frac}} \times u(mol_{CH_4}^{frac}) \right)^2 + \left(\frac{\partial x_i}{\partial mol_{EtOH}^{frac}} \times u(mol_{EtOH}^{frac}) \right)^2 + u_{rep}(x_i)^2} \quad (14)$$

Equation Substitution

Eq. 15 used to calculate mole of CH₄ in the vapor phase of the flash tank

$$mol_{CH_4}^v = (v_{CH_4} \times \rho_{CH_4}) \quad (15)$$

Eq. 16 used to calculate the mole of CH₄ in the liquid phase of the flash tank

$$mol_{CH_4}^l = \left(mol_{frac_{CH_4}}^l \times \frac{m_{EtOH}}{46} \right) \quad (16)$$

Eq. 17 used to calculate the mole of ethanol/methanol in the vapor phase of the flash tank

$$mol_{EtOH}^v = (mol_{EtOH}^{frac} \times mol_v^{CH_4}) \quad (17)$$

Eq. 18 shows the equation used to calculate the mole of ethanol in the liquid phase of the flash tank

$$mol_{EtOH}^l = \frac{m_{EtOH}}{46} \quad (18)$$

Table 5 Nomenclature

x_i	Solubility of CH ₄ in methanol/ethanol (mol/mol)
$mol_{CH_4}^v$	Mole of CH ₄ in the vapor phase
$mol_{CH_4}^l$	Mole of CH ₄ in the liquid phase
mol_{EtOH}^v	Mole of ethanol/methanol in the vapor phase
mol_{EtOH}^l	Mole of Ethanol/Methanol in the liquid phase
v_{CH_4}	Volume of CH ₄
ρ_{CH_4}	Density of CH ₄
m_{EtOH}	Mass of ethanol/methanol
$mol_{CH_4}^{frac}$	mole fraction of CH ₄ in the alcohol calculated using the CPA-SRK72 EoS.
mol_{EtOH}^{frac}	mole fraction of Ethanol/methanol in the CH ₄ (gas meter) calculated using the CPA-SRK72
$u(x_i)$	Cumulative standard uncertainty ²⁵
$u(v)$	Standard Uncertainty contribution by the gas meter volume as reported by the manufacturer
$u(m)$	Standard uncertainty contribution by the balance as reported by the manufacturer

$u(mol_{CH_4}^{frac})$	Standard uncertainty contribution by the mole fraction CPA-SRK72 (optimized) calculation of CH ₄ in the liquid phase
$u(mol_{EtOH}^{frac})$	Standard uncertainty contribution by the mole fraction CPA-SRK72 (optimized – limited data) calculation of alcohol in the vapor phase

AUTHOR INFORMATION

Corresponding Author

* Antonin Chapoy

Hydrates, Flow Assurance & Phase Equilibria, Institute of Petroleum Engineering, Heriot Watt University, EH14 4AS

Tel: +44 (0)131 451 3797

Fax: +44 (0)131 451 3539

Email: Antonin.chapoy@pet.hw.ac.uk

Present Addresses

* Hydrates, Flow Assurance & Phase Equilibria, Institute of Petroleum Engineering, Heriot Watt University, EH14 4AS

Author Contributions

The manuscript was written through contributions of all authors. All authors have given approval to the final version of the manuscript. These authors contributed equally.

Funding Sources

This project was funded through a Joint Industrial Project being conducted at the Institute of Petroleum Engineering, Heriot Watt University. The author would like to thank Chevron, GDF, Petrobras, Statoil and Total for their support of the project. I would also like to thank EPSRC for their support.

ACKNOWLEDGMENT

The author would like to thank Jim Allison, the team's technician and Dr. Jinhai Yang for all the assistance provided.

References

- (1) Yarym-agaev, N. .; Sinyavskaya R.P, K. фазовые равновесия в бинарных системах вода-метан, метанол-метан при высоких давлениях (Phase equilibria in binary systems of water-methane, methanol-methane at high pressures). *ZHurnal prikladoi Khimii* **1985**, 58, 165.
- (2) Brunner, E.; Hültenschmidt, W.; Schlichthärle, G. Fluid mixtures at high pressures IV. Isothermal phase equilibria in binary mixtures consisting of (methanol + hydrogen or nitrogen or methane or carbon monoxide or carbon dioxide). *J. Chem. Thermodyn.* **1987**, 19, 273–291.
- (3) Hong, J. H.; Malone, P. V.; Jett, M. D.; Kobayashi, R. The measurement and interpretation of the fluid-phase equilibria of a normal fluid in a hydrogen bonding solvent: the methane - methanol system. *Fluid Phase Equilib.* **1987**, 38, 83–96.
- (4) Schneider, R. PhD Thesis: Experimentelle Bestimmung der dynamischen Viskosität von Flüssigkeitsgemischen aus Methanol mit CO₂, CH₄, C₂H₆ und C₃H₈, Technical University of Berlin, 1978.
- (5) Ukai, T.; Kodama, D.; Miyazaki, J.; Kato, M. Solubility of Methane in Alcohols and Saturated Density at 280.15 K. *J. Chem. Eng. Data* **2002**, 47, 1320–1323.
- (6) Wang, L.-K.; Chen, G.-J.; Han, G.-H.; Guo, X.-Q.; Guo, T.-M. Experimental study on the solubility of natural gas components in water with or without hydrate inhibitor. *Fluid Phase Equilib.* **2003**, 207, 143–154.
- (7) Frost, M.; Karakatsani, E.; von Solms, N.; Richon, D.; Kontogeorgis, G. M. Vapor–Liquid Equilibrium of Methane with Water and Methanol. Measurements and Modeling. *J. Chem. Eng. Data* **2014**, 59, 961–967.
- (8) Suzuki, K.; Sue, H.; Itou, M.; Smith, R. L.; Inomata, H.; Arai, K.; Saito, S. Isothermal vapor-liquid equilibrium data for binary systems at high pressures: carbon dioxide-methanol, carbon dioxide-ethanol, carbon dioxide-1-propanol, methane-ethanol, methane-1-propanol, ethane-ethanol, and ethane-1-propanol systems. *J. Chem. Eng. Data* **1990**, 35, 63–66.
- (9) Brunner, E.; Hültenschmidt, W. Fluid mixtures at high pressures VIII. Isothermal phase equilibria in the binary mixtures: (ethanol + hydrogen or methane or ethane). *J. Chem.*

Thermodyn. **1990**, 22, 73–84.

- (10) Friend, D. G.; Frurip, D. J.; Lemmon, E. W.; Morrison, R. E.; Olson, J. D.; Wilson, L. C. Establishing benchmarks for the Second Industrial Fluids Simulation Challenge. *Fluid Phase Equilib.* **2005**, 236, 15–24.
- (11) Lundstrøm, C.; Michelsen, M. L.; Kontogeorgis, G. M.; Pedersen, K. S.; Sørensen, H. Comparison of the SRK and CPA equations of state for physical properties of water and methanol. *Fluid Phase Equilib.* **2006**, 247, 149–157.
- (12) Zerpa, L. E.; Sloan, E. D.; Koh, C.; Sum, A. Hydrate Risk Assessment and Restart-Procedure Optimization of an Offshore Well Using a Transient Hydrate Prediction Model. *Oil Gas Facil.* **2013**, 1, 49–56.
- (13) Ferreira, P. A.; Bezerra, M. F. C.; Loschiavo, R. The Internal Corrosion Integrity Strategy on the Development of New Offshore Production Areas in Brazil. In *Offshore Technology Conference*; Offshore Technology Conference, 2013.
- (14) Altoe Ferreira, P. The Internal Corrosion Integrity Strategy on the Development of New Offshore Production Areas in Brazil. *SPE Prod. Facil.* **2013**, 20, 324–333.
- (15) Chapoy, A.; Nazeri, M.; Kapateh, M.; Burgass, R.; Coquelet, C.; Tohidi, B. Effect of impurities on thermophysical properties and phase behaviour of a CO₂-rich system in CCS. *Int. J. Greenh. Gas Control* **2013**, 19, 92–100.
- (16) Haghighi, H.; Chapoy, A.; Burgess, R.; Mazloun, S.; Tohidi, B. Phase equilibria for petroleum reservoir fluids containing water and aqueous methanol solutions: Experimental measurements and modelling using the CPA equation of state. *Fluid Phase Equilib.* **2009**, 278, 109–116.
- (17) Haghighi, H.; Chapoy, A.; Burgess, R.; Tohidi, B. Experimental and thermodynamic modelling of systems containing water and ethylene glycol: Application to flow assurance and gas processing. *Fluid Phase Equilib.* **2009**, 276, 24–30.
- (18) Anderson, R.; Chapoy, A.; Haghighi, H.; Tohidi, B. Binary Ethanol–Methane Clathrate Hydrate Formation in the System CH₄–C₂H₅OH–H₂O: Phase Equilibria and Compositional Analyses. *J. Phys. Chem. C* **2009**, 113, 12602–12607.
- (19) Kontogeorgis, G. M.; Voutsas, E. C.; Yakoumis, I. V.; Tassios, D. P. An Equation of State

- for Associating Fluids. *Ind. Eng. Chem. Res.* **1996**, 35, 4310–4318.
- (20) Soave, G. Equilibrium constants from a modified Redlich-Kwong equation of state. *Chem. Eng. Sci.* **1972**, 27, 1197–1203.
- (21) Kontogeorgis, G. M.; V. Yakoumis, I.; Meijer, H.; Hendriks, E.; Moorwood, T. Multicomponent phase equilibrium calculations for water–methanol–alkane mixtures. *Fluid Phase Equilib.* **1999**, 158-160, 201–209.
- (22) Chapoy, A.; Mohammadi, A. H.; Richon, D.; Tohidi, B. Gas solubility measurement and modeling for methane–water and methane–ethane–n-butane–water systems at low temperature conditions. *Fluid Phase Equilib.* **2004**, 220, 111–119.
- (23) Hemmaplardh, B.; King, A. D. Solubility of methanol in compressed nitrogen, argon, methane, ethylene, ethane, carbon dioxide, and nitrous oxide. Evidence for association of carbon dioxide with methanol in the gas phase. *J. Phys. Chem.* **1972**, 76, 2170–2175.
- (24) Krichevsky, I.; Koroleva, M. The solubility of methanol in compressed gases. *Acta Physicochim. URSS* **1941**, 15, 327–342.
- (25) Taylor, B. N.; Kuyatt, C. E. *Guidelines for Evaluating and Expressing the Uncertainty of NIST Measurement Results*; 1994.

For Table of Contents Only

